

Modelling, Optimization And Prediction Of Sorption Of Pb(II) And Mn(II) Ions From Wastewater Onto Acid Activated Shale Using Adaptive Neuro Fuzzy Inference Systems (ANFIS), Response Surface Methodology (RSM) and Modular Neural Network (MNN)

I.R. Ilaboya*[‡], O.C. Izinyon**

Department of Civil Engineering, Faculty of Engineering, University of Benin, P.M.B 1154

* Benin City, Edo State, Nigeria

Corresponding Author: Email; rudolph.ilaboya@uniben.edu Mobile No: +2348038027260

Received: 29.11.2018 Accepted: 26.03.2020

Abstract- Batch experimental technique was employed to evaluate the effects of adsorption variables such as initial metal ion concentration, adsorbent dose, pH, and contact time on the sorption efficiency of Pb(II) and Mn(II) ions onto acid activated shale. To select the input variables with the highest significant contributions towards the sorption of Pb(II) and Mn(II) ions onto acid activated shale, adaptive neuro-fuzzy (ANFIS) was employed. Thereafter, statistical design of experiment (DOE) using central composite design was used to generate the data for modelling and prediction using a modular neural network (MNN). To produce accurate network architecture for prediction, the input data were first normalized to avoid the problems of weight variation. Thereafter, different training algorithm and hidden neurons were selected and tested to ascertain the optimum number of hidden neuron and the best training algorithm that will produce the most accurate network. The linear coefficient of determination in addition to the mean square error for training and cross-validation was employed as the selection criteria. Results obtained shows that, Levenberg Marquardt Back Propagation training algorithm with 2 hidden neurons in the input and output layer with tangent sigmoid transfer function produced the most accurate prediction network. In addition, the modular neural network gave a strong agreement between the experimental and predicted sorption efficiency of Pb(II) and Mn(II) ions with R² values of 0.977 and 0.9648 having performance statistics of RMSE (0.03815), NRMSE (0.04097), Max.AE (0.02621), Min.AE (0.00041) and R² (0.988).

Keywords: Modular neural network, sensitivity analysis, Response surface methodology, central composite design, Adaptive neuro-fuzzy inference system

Özet- Başlangıç metal iyonu konsantrasyonu, adsorban dozu, pH ve temas süresi gibi adsorpsiyon değişkenlerinin Pb (II) ve Mn (II) iyonlarının asitle aktifleştirilmiş şeyl üzerindeki sorpsiyon verimliliği üzerindeki etkilerini değerlendirmek için seri deneysel teknik kullanılmıştır. Asit aktive edilmiş şeyl üzerine Pb (II) ve Mn (II) iyonlarının sorpsiyonuna en önemli katkıları olan girdi değişkenlerini seçmek için adaptif nöro-bulanık (ANFIS) kullanılmıştır. Daha sonra, modüler bir sinir ağı (MNN) kullanılarak modelleme ve tahmin için veri üretmek üzere merkezi kompozit tasarım kullanılarak deney (DOE) istatistiksel tasarımı kullanıldı. Tahmin için doğru ağ mimarisi üretmek üzere, giriş verileri önce ağırlık değişimi problemlerinden kaçınmak için normalleştirilmiştir. Daha sonra, optimum gizli nöron sayısını ve en doğru ağı üretecek en iyi eğitim algoritmasını belirlemek için farklı eğitim algoritması ve gizli nöronlar seçildi ve test edildi. Seçim kriterleri olarak eğitim ve çapraz validasyon için ortalama kare hataya ek olarak, doğrusal belirleme katsayısı kullanılmıştır. Elde edilen sonuçlar, teğet sigmoid transfer fonksiyonu ile giriş ve çıkış katmanında 2 gizli nöron içeren Levenberg Marquardt Geri Yayılım eğitim algoritmasının en doğru tahmin ağını ürettiğini göstermektedir. Ek olarak, modüler sinir ağı, R² değeri 0.977 ve 0.9648 R² arasında olan ve RMSE (0.03815), NRMSE (0.04097), Max.AE (0.02621), Min.AE (0.00041) ve R² (0.988) performans istatistiğine sahip Pb (II) ve Mn (II) iyonlarının deneysel ve tahmin edilen sorpsiyon verimliliği arasında güçlü bir uyum sağlamıştır.

Anahtar Kelimeler Modüler sinir ağı, duyarlılık analizi, yanıt yüzeyi metodolojisi, merkezi kompozit tasarım, uyarlanabilir nöro-bulanık çıkarım sistemi.

1. Introduction

Environmental pollution caused by the discharge of untreated effluents containing toxic metals such as lead, chromium, and manganese has become an issue of concern and have developed into a widely studied area (1). Unlike organic pollutants, the majority of which are susceptible to biological degradation, heavy metals will not degrade into harmless end products, and their presence in streams and lakes leads to bioaccumulation in living organisms, causing health problems in animals, plants and human beings (2).

Some conventional processes have been developed over the years to remove these heavy metals from water and wastewater they include; solvent extraction, chemical precipitation, ion exchange process, electrolytic precipitation, and reverse osmosis (3).

However, these physicochemical processes possess significant limitations of being highly expensive, sophisticated and environmentally disruptive, requiring the input of external chemical additives or energy. In addition, some of these conventional processes especially electrolytic and chemical precipitations generate concentrated sludge or another kind of waste that must be properly disposed to avoid further damage to the environment (4, 5).

Adsorption is an alternative technology for metal separation from aqueous solutions. With the selection of a proper adsorbent, the adsorption process can be a promising technique for the removal of certain types of contaminants including heavy metals (6). However, since the adsorption process is influenced by different variables which are not linearly related, traditional methods of data generation and processing are no longer suitable in solving adsorption related issues such as determination of optimum values of adsorption variables and prediction of sorption efficiency of metal ions on porous solid adsorbent.

In recent years, statistical design of experiment (DOE) and artificial neural network (ANN) has been successfully employed to optimize and predict the sorption efficiency of divalent metals on different adsorbents such as zeolite (7), electric arc furnace slag (8), sunflower powder (9), Zea Mays (10), *Aspergillus terreus* biomass (11). In their various studies, the authors generated large volume of experimental data using statistical design of experiment employing either the 2-level factorial design or the full factorial central composite design. The experimental data were then used as input data for ANN modelling from which 60% was employed for training the network, 20% was used for validating the network and the remaining 20% was employed for testing the network.

Although, artificial neural network (ANN) are one of the many machine learning tools that are capable of performing the task of modeling and prediction of experimental data, the large amount of dimensionality both in terms of the number of features the data has, as well as the number of rows of data the network is to handle tends to increase the required training circle and time thereby reducing the accuracy of prediction (12). Following this, modular neural network (MNN) was

employed since they represent a special class of multi-layer perceptron neural network (MLP) which process their input using several parallel MLPs and then recombine the results thus creating some structure within the network topology which will foster specialization of function in each sub-module. This tends to speed up the learning rate, training times and reduce the number of required training circles thereby producing a more accurate result.

Shale was used as adsorbent for this study because it is a fine-grained particle. The size of its particles gives it the needed high surface area for metal ion adsorption.

2. Brief description of modelling, optimization and prediction techniques

2.1. Adaptive Neuro-fuzzy Inference Systems

The complexity of real life problems require modern methods for the construction of knowledge systems that can be used in the solution to such problems. The search for systems that can solve increasingly complex problems has initiated research in a number of scientific fields, especially Hybrid Intelligent Systems. This area tends to combine different techniques of learning and adaptation to overcome their individual challenges. One of such hybrid systems is Neuro-Fuzzy approach that can learn from the environment and then reason about its state. Adaptive Neuro-fuzzy systems constitute an intelligent hybrid technique that combines fuzzy logic with neural networks in order to have better results. While the learning capability is an advantage provided by artificial neural network, the formation of a linguistic rule base is an advantage provided by the fuzzy inference system.

2.2. Response Surface Methodology

Response surface methodology (RSM) is an array of statistical and mathematical techniques, employed for developing, modelling and analyzing processes in which several variables influenced a response of interest and the main objective is to optimize the response (13). They are used in industries to

- i. Explore the relationship between a response variable and several input variables
- ii. Determine the optimal settings of the variables, and
- iii. Optimize the process.

They are mostly applied in situations where there are many input variables that may influence one or more response variables and are used to develop an empirical model commonly called response surface (14, 15). Response Surface Methodology (RSM) allows you to specify and fit a polynomial model up to second order and provides an option to include a block variable when the need arises.

2.3. Modular Neural Network

Modular feed forward networks are a special class of multi-layer perceptron neural network (MLP). These networks process their input using several parallel MLPs, and then recombine the results. This tends to create some structure within the topology, which will foster specialization of function in each sub-module. In contrast to the MLP, modular networks do not have full interconnectivity between their layers. Therefore, a smaller number of weights are required for the same size of network. This tends to speed up training times and reduce the number of required training circles.

3. Research Methodology

3.1 Collection and Preparation of Adsorbent

Shale was collected from its deposit at Okada the administrative headquarter of Ovia North East Local Govt. Area of Edo State, Nigeria. First, it was soaked in a plastic containing 5% hydrogen peroxide to remove any carbonaceous matter that can interfere with the metal adsorption capacity of the shale. Thereafter, it was washed with distilled water to remove any water soluble impurities before being dried in hot air oven at 50-70°C for 8 hours. The dried shale was then reduced to fine and sieved using sieve size of 212µm before use (16, 17).

For acid activation, 500g of the dried sieved shale mineral was placed in a furnace at a temperature of 550 OC for 10 hours. 200 g of the calcinated shale mineral was then mixed with 1 liter 0.25M sulphuric acid, the mixture was heated at 105°C for 30 minutes. After slow cooling, the slurry was filtered and washed free of acid using distilled water as indicated by a pH meter. The shale was dried at a temperature of 100°C for 30 – 45 minutes, ground using mortar and pestle, sieved to 212 µm and stored in a desiccator to cool before use (1)

3.2 Characterization of adsorbent

3.2.1. Analysis of Microstructures

The microstructure of shale was analyzed using scanning electron microscopy (APEX 3020 PSEM 2) to give adequate information about its morphology and topological presentations. Such presentations provided possible explanations of the solid behaviour (18).

3.2.2. Chemical composition

The chemical composition of shale was studied using X-Ray Fluorescence (XRF) APEX 3022. Chemical digestion of the solid adsorbent was done as follows: (1:1) mixture of 0.025M solution of hydrochloric acid and Nitric acid was prepared. A mixture of (1:10) of the solid adsorbent to acid solution was obtained and stir for 30 minutes. The solution was filtered and the filtrate was used for the analysis (19).

3.3 Preparation of aqueous solution

All the chemicals used in this research were analytical grade. Stock solution of lead and manganese were prepared by dissolving accurate quantities of lead (II) nitrate [Pb (NO₃)₂], manganese (II) chloride tetrahydrate (MnCl₂·4H₂O) in one liter of distilled water. All working solutions were obtained by diluting the stock solution with distilled water and the concentration of metal ion present in solution was analyzed by Atomic Absorption Spectrophotometer. A duplicate was analyzed for each sample to track experimental error and show capability of reproducing results. The pH of the solution was adjusted to the desired values for each experiment with drop wise addition of 1M HNO₃ or 1M NaOH.

3.4 Adsorption studies

Adsorption study was carried out to determine the effect of pH, adsorbent dose, adsorption temperature, contact time and initial metal ion concentration using batch adsorption technique. The adsorption experiment were performed at different variable range as follows; pH (2, 4, 6, 8, and 10), adsorbent dose (0.2, 0.4, 0.6, 0.8 and 1.0g), contact time (20, 40, 60, 80, 100, and 120 minutes), adsorption temperature (288, 293, 298, 303 and 308K) and different initial metal ion concentration. A 250ml conical flask containing the adsorbent and 50ml aqueous solution of the metal was agitated at 150rpm using a mantle fitted with magnetic stirrer. The pH values of the aqueous solutions were kept at the optimum for each heavy metal.

The separation of the adsorbent and aqueous solution of heavy metals was carried out by filtration with 150mm whatman filter paper and the filtrates were stored in sample cans in a refrigerator prior to analysis. The residual metal ion concentration were also determined using an Atomic Absorption Spectrophotometer (AAS)

The amount of heavy metal ions removed during the series of batch investigation was determined using the mass balance equation of the form; (20).

$$q = \frac{V}{m} [C_0 - C_e] \quad (3.1)$$

Where: q, defines the metal uptake (mg/g); C₀ and C_e: are the initial and equilibrium metal ion concentrations in the aqueous solution [mg/l] respectively; V: is the aqueous sample volume (ml) and m: is the mass of adsorbent used (g). The efficiency of metal ion removal (%) was calculated using the mass balance equation of the form;

$$\text{Efficiency (\%)} = \left(\frac{C_0 - C_e}{C_0} \times 100 \right) \quad (3.2)$$

Where: C₀ and C_e are the metal ion concentrations (mg/l) in aqueous solution before and after adsorption respectively.

3.5 Data generation using design of experiment (DOE)

The range and levels of the experimental variables used for the design are presented in Table 3.1 and 3.2

3.5.1 Screening of experimental variables using Anfis

Adsorption of Pb(II) and Mn(II) ions onto shale is influenced by numerous adsorption variables such as; adsorption temperature, pH, adsorbent dose, contact time and initial metal ion concentration. To optimize the adsorption process, there was need to first screen the variables so as to select those variables with the highest significant effects on the overall process of adsorption.

To perform the variable screening, design of experiment (DOE) was done to generate the input data while adaptive neuro-fuzzy inference systems (ANFIS) was employed to train a fuzzy inference systems (FIS) structure which was thereafter employed to screen the variables based on there error variance. Variables with the least error variance were selected as the most significant variables. To train the fuzzy inference systems (FIS) structure, 2⁵-level factorial design of experiment with two replicates, one block and four center points resulting to seventy two (72) experimental runs based

Table 3.1: Levels of independent variables for Pb(II) ion adsorption

Independent Variable	Range and Level				
	-2	-1	0	+1	+2
Initial Metal Ion Conc. (Mg/l): X ₁	5	10	15	20	25
pH: X ₂	2	4	6	8	10
Adsorption Temperature (K): X ₃	288	293	298	303	308
Adsorbent Loading (g): X ₄	0.2	0.4	0.6	0.8	1.0
Contact Time (min) X ₅	24	48	72	96	120

Table 3.2: Levels of independent variables for Mn(II) ion adsorption

Independent Variable	Range and Level				
	-2	-1	0	+1	+2
Initial Metal Ion Conc. (Mg/l): X ₁	4	8	12	16	20
pH: X ₂	2	4	6	8	10
Adsorption Temperature (K): X ₃	288	293	298	303	308
Adsorbent Loading (g): X ₄	0.2	0.4	0.6	0.8	1.0
Contact Time (min) X ₅	24	48	72	96	120

on Pb(II) ion adsorption onto shale was used to generate the input data for which 60% was used for training, 25% for validation, and 15% for checking. An error tolerance of 0.5, 40 epochs and a hybrid method of optimization were selected to improve the performance of the FIS structure. The initial model parameters required for training a fuzzy inference systems (FIS) structure were sub-divided into

1. input_name (data set generated from 2⁵-level factorial design of experiment)
2. trn_data (60% of input_name)
3. chk_data (40% of input_name)

The data were then presented to MATLAB as presented in figure 3.1a

```
>> a = 'initial metal ion concentration';
>> b = 'pH';
>> c = 'adsorption temperature';
>> d = 'adsorbent loading';
>> e = 'contact time';
>> f = 'percent removal of heavy metal';
>> input_name = char(a, b, c, d, e, f);
>> a = [x1; x2; x3; x4; x5];
>> b = [x1; x2; x3; x4; x5];
>> c = [x1; x2; x3; x4; x5];
>> d = [x1; x2; x3; x4; x5];
>> e = [x1; x2; x3; x4; x5];
>> f = [x1; x2; x3; x4; x5];
>> input_data = [a b c d e f];
```

Figure 3.1a: Anfis input data format

The initial input parameters were then subdivided into training and checking data as presented in figure 3.1b

```
>> tm_data_n = k
>> tm_data = input_data (1:tm_data_n, :);
>> chk_data = input_data (tm_data_n+1: tm_data_n+p, :);
```

Figure 3.1b: Subdivision of training and checking data

Training of data set allows you to check the generalization capability of the resulting fuzzy inference systems (FIS). To perform the data training, the program presented in figure 3.1c was employed

```
>> load tm_data
>> load tm_data
>> anfisfit
```

Figure 3.1c: Anfis training program

To find the single and combine adsorption variable(s) with the highest significant contributions, the program in figure 3.1d was employed

```
>> exhsrch (1, tm_data, chk_data, input_data);
>> exhsrch (2, tm_data, chk_data, input_data);
>> exhsrch (3, tm_data, chk_data, input_data);
```

Figure 3.1d: Anfis search program

For Mn(II) ion adsorption onto shale, 2^{n-1} -level factorial design of experiment with one replicates, one block and four center points resulting to twenty experimental runs was employed to generate the input data which were first validated using the trained FIS structure for Pb(II) ion adsorption before been modeled for the variable screening process.

3.5.2 Adsorption process optimization using RSM

For Pb(II) ion adsorption, different initial metal ion concentration of 5 – 25mg/l, varied adsorbent dose of 0.2 – 1.0g, different pH of 2 – 10 and different contact time of 24 – 120mins for a constant adsorption temperature of $27\pm 2^{\circ}\text{C}$ was used. For Mn(II) ion adsorption, different initial metal ion concentration of 4 – 20mg/l, varied adsorbent dose of 0.2 – 1.0g, different pH of 2 – 10 and different contact time of 24 – 120mins for a constant adsorption temperature of $27\pm 2^{\circ}\text{C}$ was used. These variables were coupled together and varied simultaneously to cover the combination of parameters proposed by the CCD. The level and ranges of the selected variables were randomized using design expert software. A full factorial CCD design comprising of sixteen factorial points, eight axial points and six replicates at the center point resulting in a total of 30 experimental runs as shown in Table 3.2a and 3.2b was employed to optimize the selected variables

Table 3.2a: Central composite design matrix showing coded and real variables with observed and predicted Pb(II) ion adsorption onto acid activated shale

Experimental Runs	Coded Values of Variables				Real Values of Variables				Pb(II) Sorption Efficiency (%)	
	X ₁ (mg/l)	X ₂ (pH)	X ₃ (g/l)	X ₄ (mins)	X ₁ (mg/l)	X ₂ (pH)	X ₃ (g/l)	X ₄ (mins)	Observed	RSM Predicted
1	0	0	0	0	15.000	6.000	0.600	72.000	88.6	89.64
2	0	0	0	0	15.000	6.000	0.600	72.000	88.8	89.64
3	0	0	0	0	15.000	6.000	0.600	72.000	87.9	89.64
4	0	0	0	0	15.000	6.000	0.600	72.000	88.7	89.64
5	0	0	0	0	15.000	6.000	0.600	72.000	88.7	85.52
6	0	0	0	0	15.000	6.000	0.600	72.000	88.7	85.52
7	0	+1	0	0	15.000	8.000	0.600	72.000	89.6	88.39
8	0	0	0	+2	15.000	6.000	0.600	120.00	54.6	56.90
9	0	+2	0	0	15.000	10.00	0.600	72.000	68.7	69.72
10	0	0	-2	0	15.000	6.000	0.200	72.000	76.3	76.37
11	0	0	+2	0	15.000	6.000	1.000	72.000	79.1	76.24
12	0	0	0	-2	15.000	6.000	0.600	24.000	71.5	75.45
13	+2	0	0	0	25.000	6.000	0.600	72.000	72.6	72.52
14	-1	0	0	0	10.000	6.000	0.600	72.000	86.7	87.87
15	-2	+2	-2	+2	5.0000	10.00	0.200	120.00	87.5	88.19
16	+2	+2	+2	-2	25.000	10.00	1.000	24.000	65.7	65.76

17	-2	+2	-2	-2	5.0000	10.00	0.200	24.000	89.7	91.28
18	+2	+2	+2	+2	25.000	10.00	1.000	120.00	65.4	66.02
19	+2	-2	+2	+2	25.000	2.000	1.000	120.00	76.5	77.31
20	-2	-2	-2	-2	5.0000	2.000	0.200	24.000	64.5	62.01
21	-2	+2	+2	-2	5.0000	10.00	1.000	24.000	88.4	86.62
22	+2	-2	-2	-2	25.000	2.000	0.200	24.000	68.9	68.49
23	+2	+2	-2	-2	25.000	10.00	0.200	24.000	88.7	88.98
24	-2	-2	+2	-2	5.0000	2.000	1.000	24.000	74.8	75.62
25	-2	+2	+2	+2	5.0000	10.00	1.000	120.00	87.6	89.14
26	+2	+2	-2	+2	25.000	10.00	0.200	120.00	73.9	72.96
27	-2	-2	-2	+2	5.0000	2.000	0.200	120.00	87.3	85.72
28	+2	-2	-2	+2	25.000	2.000	0.200	120.00	81.2	79.49
29	+2	-2	+2	-2	25.000	2.000	1.000	24.000	92.3	92.11
30	-2	-2	+2	+2	5.0000	2.000	1.000	120.00	84.7	83.06

Table 3.2b: Central composite design matrix showing coded and real variables with observed and predicted Mn(II) ion adsorption onto acid activated shale

Experimental Runs	Coded Values of Variables				Real Values of Variables				Mn(II) Sorption Efficiency (%)	
	X ₁ (mg/l)	X ₂ (g/l)	X ₃ (pH)	X ₄ (mins)	X ₁ (mg/l)	X ₂ (g/l)	X ₃ (pH)	X ₄ (mins)	Observed	RSM Predicted
1	0	0	0	0	12.00	0.600	6.000	72.000	76.5	76.36
2	0	0	0	0	12.00	0.600	6.000	72.000	76.4	76.36
3	0	0	0	0	12.00	0.600	6.000	72.000	76.4	76.36
4	0	0	0	0	12.00	0.600	6.000	72.000	76.5	76.36
5	0	0	0	0	12.00	0.600	6.000	72.000	76.3	74.93
6	0	0	0	0	12.00	0.600	6.000	72.000	76.4	74.93
7	0	-2	0	0	12.00	0.200	6.000	72.000	75.8	74.80
8	0	+1	0	0	12.00	0.800	6.000	72.000	64.3	65.71
9	0	0	+1	0	12.00	0.600	8.000	72.000	74.3	73.41
10	0	0	-2	0	12.00	0.600	2.000	72.000	75.3	76.60
11	0	0	0	+1	12.00	0.600	6.000	96.000	65.2	64.48
12	0	0	0	-2	12.00	0.600	6.000	24.000	66.7	67.83
13	-1	0	0	0	8.000	0.600	6.000	72.000	67.1	63.33
14	-2	0	0	0	4.000	0.600	6.000	72.000	83.7	87.88
15	+2	+2	-2	+2	20.00	1.000	2.000	120.00	65.4	66.58
16	+2	+2	-2	-2	20.00	1.000	2.000	24.000	63.2	65.22
17	-2	-2	+2	-2	4.000	0.200	10.00	24.000	67.5	66.31
18	+2	-2	+2	+2	20.00	0.200	10.00	120.00	64.5	66.98
19	+2	-2	-2	-2	20.00	0.200	2.000	24.000	71.2	73.34
20	-2	+2	-2	+2	4.000	1.000	2.000	120.00	65.4	64.71
21	-2	-2	+2	+2	4.000	0.200	10.00	120.00	67.3	69.95
22	+2	+2	+2	-2	20.00	1.000	10.00	24.000	64.8	63.34
23	-2	+2	+2	-2	4.000	1.000	10.00	24.000	76.8	76.89
24	-2	-2	-2	-2	4.000	0.200	2.000	24.000	76.1	74.41
25	-2	+2	-2	-2	4.000	1.000	2.000	24.000	79.8	81.45
26	+2	+2	+2	+2	20.00	1.000	10.00	120.00	84.5	80.99
27	+2	-2	-2	+2	20.00	0.200	2.000	120.00	85.4	83.88
28	+2	-2	+2	-2	20.00	0.200	10.00	24.000	74.3	74.12
29	-2	-2	-2	+2	4.000	0.200	2.000	120.00	88.7	85.31
30	-2	+2	+2	+2	4.000	1.000	10.00	120.00	77.8	77.58

The behaviour of the system which was used to evaluate the relationship between the response variable (y) and the independent variables X₁, X₂, X₃ and X₄ was explained using

the empirical second-order polynomial model depicted by equation (3.3)

$$Y = \beta_0 + \sum_{i=1}^q \beta_i x_i + \sum_{i=1}^q \beta_{ii} x_i^2 + \sum_{i=1, i < j=2}^{q-1} \sum_{j=2}^q \beta_{ij} x_i x_j + \varepsilon \quad (3.3)$$

Where $X_1, X_2, X_3 \dots X_k$ are the input variables which affect the response, $Y, \beta_0, \beta_i, \beta_{ii}$, and β_{ij} , ($i = 1-k, j = 1-k$) are the known parameters and ε is the random error.

To assess the model significance and justify the potential of response surface methodology (rsm) in optimizing the adsorption variables, one way analysis of variance was used. Reliability of the ANOVA result was judged using the fisher's F value and the probability function ($P < 0.05$). Large value of F corresponding to very low value of P ($P \ll 0.05$) was used to determine the level of significance of the model. The adequacy of rsm model and the reliability of the resulting second order polynomial equation were assessed using the goodness of fit statistics, namely; coefficient of determination (R^2), adjusted (R-squared) value and adequate precision value.

3.5.3 Data analysis and prediction using Modular neural network

For modular neural network modelling, each layer of parameters usually contains a vector of processing elements (PEs) and the parameters selected apply to the entire vector. The parameters are dependent on the neural model, but all require a nonlinearity function to specify the behaviour of the PEs. In addition, each layer has an associated learning rule and learning parameters. Note that the number of PEs for the output layer is determined by the number of columns selected as your desired response.

3.5.3.1 Input data generation and processing

Input data employed for the training, validation and testing were gotten from series of batch experiments based on central composite design of experiment under varied initial metal ion concentration, pH, adsorbent dose and contact time. A full factorial central composite design of experiment with 6 center points and 3 replicates resulted in a total of 90 experimental runs were used as the input data. The data were randomly divided into three subsets to represent the training (60%), validation (25%) and testing (15%). The validation data was employed to assess the performance and the generalization potential of the trained network while the testing data was to test the quality of the trained network.

To avoid the problem of weight variation which can subsequently affects the efficiency of the training process, the input and output data were first normalized to a give a weight between 0.1 and 1.0 using visual developer (7).

3.5.3.2 Data training and design of network architecture

Input data training resulting to design of network architecture is of paramount importance in the application of neural network to data modeling and prediction. To obtain the optimal network architecture that possesses the most accurate

understanding of the input data, two factors were considered. First was the selection of the most accurate training algorithm and secondly, the number of hidden neuron.

Based on this consideration, different training algorithm were selected and tested to determine the best training algorithm that will produce the most accurate network architecture. Thereafter different hidden neurons were selected based on the most accurate training algorithm to determine the exact number of hidden neurons.

3.5.3.3 Network training and performance of modular neural network

To train the network, 3 runs of 1000 epochs each were used. In addition, cross validation data representing about 15% of the total input data were introduced to monitor the training process and prevent the network from memorizing the input data instead of leaning which was a common problem associated with overtraining. The progress of the training was checked using the mean square error of regression (MSEREG) graph for training and cross validation

3.5.3.4 Network testing and validation

To test the efficiency of the trained network, 25% of the input data representing 22 input parameters were introduced to the network. To validate the accuracy of the trained network, a linear plot of the predicted value and the observed value of Pb(II) ion sorption efficiency onto acid activated shale was obtained and the coefficient of determination R^2 value was employed as a bases for judgement.

3.5.3.5 Sensitivity analysis of modular neural network

Sensitivity analysis of the network was done to allow the trained network to assess the overall contributions of each input variables to the sorption efficiency of Pb(II) ion onto acid activated shale. Sensitivity analysis was employed to give insights into the relative importance of individual input parameters in other to identify those parameters that can be safely ignored in subsequent analysis

3.5.3.6 Network application to new data

To test the ability of the network to predict the sorption efficiency of Mn(II) ion onto acid activated shale, 30 input data generated from a response surface CCD design of experiment were normalized and presented to the network as prediction data. Comparison between the predicted sorption efficiency of manganese and the experimental values was obtained and the correlation coefficient was employed to measure the accuracy of prediction.

4. Results and discussion

4.1 Microstructural and chemical composition of shale fractions

Result of the microstructural and chemical analysis of the raw shale, calcinated and acid activated shale conducted using scanning electron microscopy (SEM) and X-Ray

Fluorescence (XRF) is presented in Figure 4.1, Figure 4.2, Figure 4.3 and Table 4.1 respectively

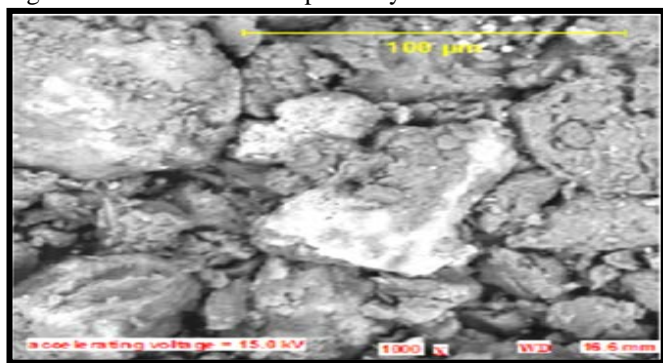


Figure 4.1: SEM of raw shale

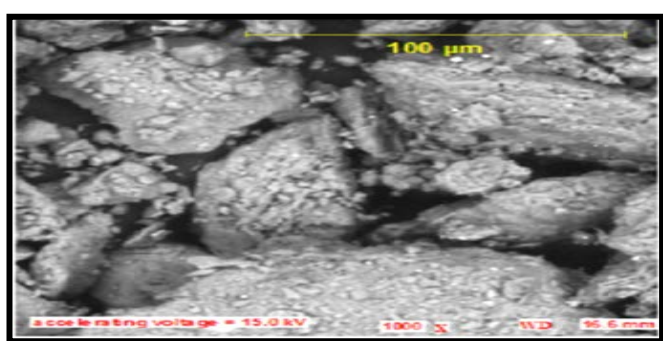


Figure 4.2: SEM of calcinated shale

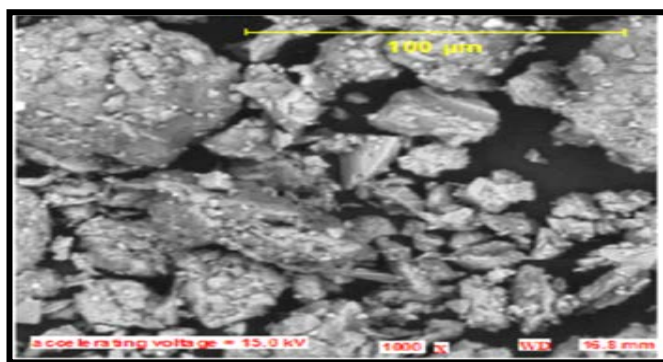


Figure 4.3: SEM of acid activated shale

Scanning electron micrograph (SEM) was taken in order to verify the presence of micropores in the structure of the shale. It was observed from Figures 4.1, 4.2 and 4.3 that the surface characteristics of the shale materials changes drastically with calcination and acid treatment with the acid treated shale showing a better irregular porous surface structure. The implication is that acid treatment tends to open up the pore spaces better than calcination thereby increasing the adsorption properties of the material. The larger number of macroporous structure seen with acid activated shale indicates a higher surface area. This claim is based on the fact that as biosorbent materials present larger numbers of microporous

structure, it adsorb higher amount of nitrogen, which resulted to a higher BET surface area as reported in (21, 22)

Scanning electron micrograph (SEM) was taken in order to verify the presence of micropores in the structure of the shale. It was observed from Figures 4.1, 4.2 and 4.3 that the surface characteristics of the shale materials changes drastically with calcination and acid treatment with the acid treated shale showing a better irregular porous surface structure. The implication is that acid treatment tends to open up the pore spaces better than calcination thereby increasing the adsorption properties of the material. The larger number of macroporous structure seen with acid activated shale indicates a higher surface area. This claim is based on the fact that as biosorbent materials present larger numbers of microporous structure, it adsorb higher amount of nitrogen, which resulted to a higher BET surface area as reported in (21, 22)

It was observed from the result of Table 4.1 that aluminium oxide and silicon oxide were the dominant oxides present in shale minerals. The alumina composition of the raw shale was observed to be 21.33wt%, it increases to 24.41wt% for the calcinated shale and decreases to 18.13wt% for the acid activated shale apparently due to the acid dealumination of the shale resulting from the effects of acidification. The high value of alumina observed with shale makes shale fraction a potential adsorbent.

Table 4.1: Chemical analysis of shale fractions

Oxides (Wt. %)	Lit. Value	RSA	CSA	AAS
SiO ₂	69.00	49.53	54.47	57.19
Al ₂ O ₃	13.33	21.33	24.41	18.13
TiO ₂	NA	1.36	1.18	2.17
Fe ₂ O ₃	2.09	2.74	2.09	0.28
MgO	3.38	1.73	1.14	1.63
MnO	NA	0.06	0.05	0.04
CaO	2.83	2.23	2.03	1.64
Na ₂ O	1.93	2.21	1.87	1.56
K ₂ O	NA	2.11	2.26	2.03
P ₂ O ₅	NA	0.54	1.23	0.32
Si/Al ₃	5.176	1.581	2.231	3.154

(RSA: Raw Shale Adsorbent) (CSA: Calcinated Shale Adsorbent) (AAS: Acid Activated Shale)

4.2 Screening of absorption variables using Anfis

An error tolerance level of 0.5, 40 epochs and a hybrid optimization method was used to generate the fis structure as shown in Figures 4.4, 4.5 and 4.6 respectively.

The adequacy of the fis structure was established from the performance error curve which shows the learning rate against the propagated error. Performance error lesser than unity implies that the fis structure is adequate. Upon validation, the performance of the fis structure was then assessed using the checking data sets. A root mean square error (rmse) value of 0.04028 was good enough to declare that the fis structure can navigate the design space and predict accurately the variables with the most significant contributions towards the adsorption process. To ascertain the variables with the highest significant contributions, a graphical variation of each independent factor variable and the corresponding root mean square error was generated as presented in Figure 4.7a-d

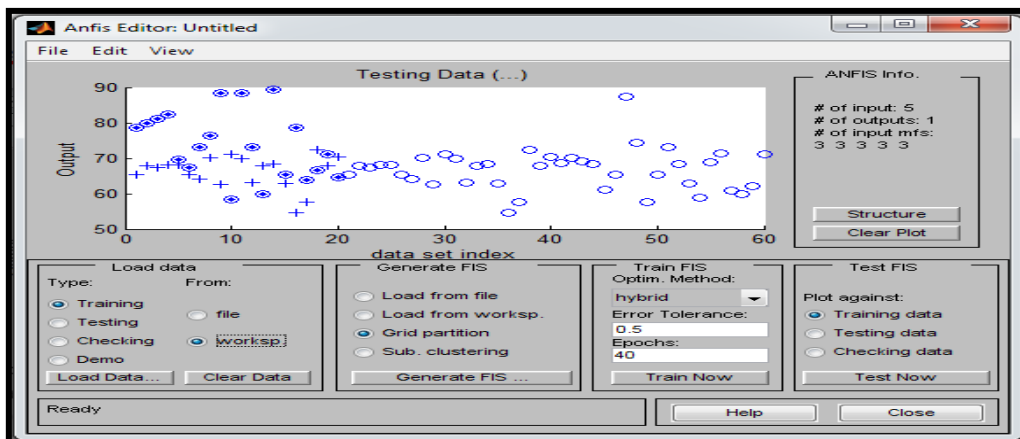


Figure 4.4: Adaptive Neuro-Fuzzy Interphase for fis structure generation

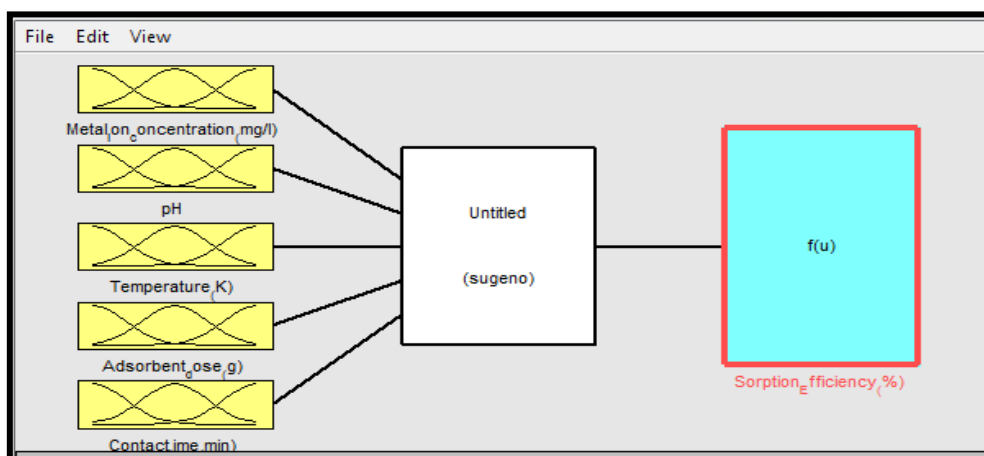


Figure 4.5: Input parameters for fis structure generation

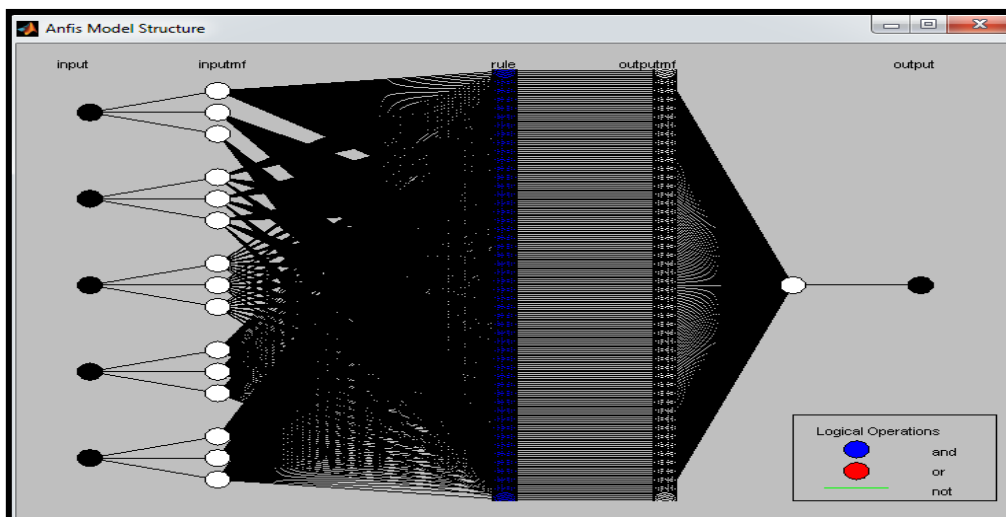


Figure 4.6: Fis structure for testing and validation of experimental data

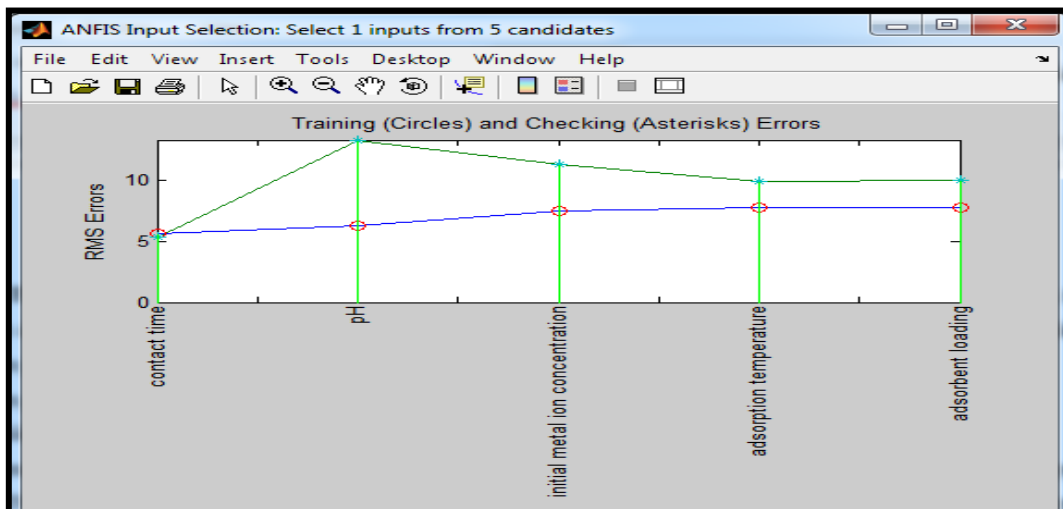


Figure 4.7a: Anfis criteria variable selection for Pb(II) ion adsorption (1 variable from 5)

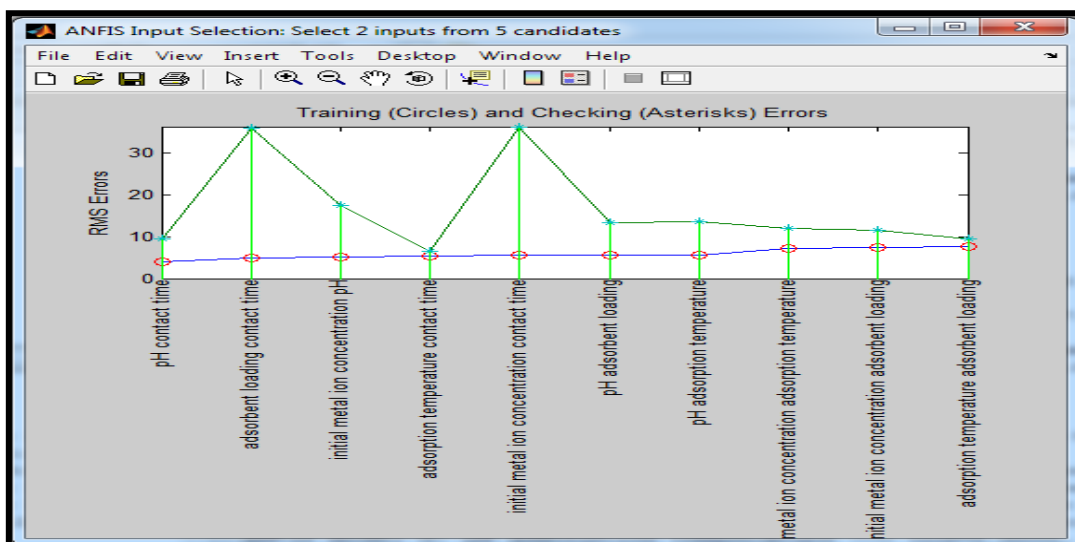


Figure 4.7b: Anfis criteria variable selection for Pb(II) ion adsorption (2 variables from 5)

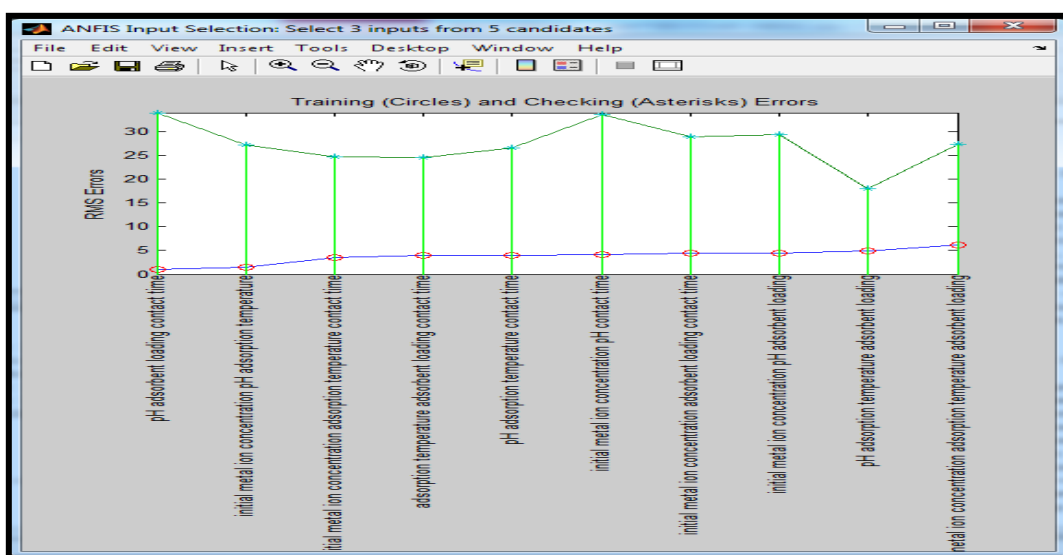


Figure 4.7c: Anfis criteria variable selection for Pb(II) ion adsorption (3 variables from 5)

From the results of Figures 4.8a-b, it was observed that initial metal ion concentration, pH of aqueous solution, adsorbent dose and contact time were the most significant variables that affect the adsorption of Mn (II) ion onto acid activated shale. Since adaptive neuro fuzzy inference system (Anfis) was able to successfully select the variables that most influenced the adsorption of each metal ion on acid activated shale, a response surface methodology (rsm) employing the central composite design (CCD) was thereafter employed to

optimize the overall process of adsorption in other to determine the optimal values of each independent variables that will bring about the most effective metal ion removal.

4.3 Adsorption process optimization using RSM, Inverse Matrix and Genetic Algorithm

Result of the one way analysis of variance (ANOVA) for the sorption of Pb(II) and Mn(II) ion onto acid activated shale are presented in Tables 4.2a-b

Table 4.2a: Analysis of variance table for validating model significance in optimizing the sorption of Pb(II) ion onto acid activated shale

Response	1	Pb(II) Sorption Efficiency			
ANOVA for Response Surface Quadratic Model					
Analysis of variance table [Partial sum of squares - Type III]					
Source	Sum of Squares	df	Mean Square	F Value	p-value Prob > F
Block	112.89	1	112.89		
Model	2715.52	14	193.97	35.94	< 0.0001 significant
A-Initial metal	1486.80	1	1486.80	275.52	< 0.0001
B-pH	66.33	1	66.33	12.29	0.0035
C-Adsorbent d	0.92	1	0.92	0.17	0.6859
D-Contact time	353.43	1	353.43	65.49	< 0.0001
AB	7.98	1	7.98	1.48	0.2441
AC	50.77	1	50.77	9.41	0.0084
AD	82.36	1	82.36	15.26	0.0016
BC	38.75	1	38.75	7.18	0.0180
BD	8.56	1	8.56	1.59	0.2286
CD	58.14	1	58.14	10.77	0.0055
A ²	284.35	1	284.35	52.69	< 0.0001
B ²	266.97	1	266.97	49.47	< 0.0001
C ²	160.61	1	160.61	29.76	< 0.0001
D ²	48.69	1	48.69	9.02	0.0095

Table 4.2b: Analysis of variance table for validating model significance in optimizing the adsorption of Mn(II) ion onto acid activated shale

Response	1	Mn(II) Sorption Efficiency			
ANOVA for Response Surface Quadratic Model					
Analysis of variance table [Partial sum of squares - Type III]					
Source	Sum of Squares	df	Mean Square	F Value	p-value Prob > F
Block	13.73	1	13.73		
Model	1317.49	14	94.11	13.03	< 0.0001 significant
A-Initial metal	123.76	1	123.76	17.13	0.0010
B-Adsorbent d	15.20	1	15.20	2.10	0.1689
C-pH	16.83	1	16.83	2.33	0.1492
D-Contact time	904.05	1	904.05	125.14	< 0.0001
AB	4.10	1	4.10	0.57	0.4637
AC	52.93	1	52.93	7.33	0.0170
AD	1.27	1	1.27	0.18	0.6819
BC	9.77	1	9.77	1.35	0.2644
BD	23.28	1	23.28	3.22	0.0942
CD	0.051	1	0.051	7.008E-003	0.9345
A ²	37.40	1	37.40	5.18	0.0391
B ²	0.011	1	0.011	1.487E-003	0.9698
C ²	131.88	1	131.88	18.25	0.0008
D ²	0.79	1	0.79	0.11	0.7457

The goodness of fit statistics used in validating the significance of the model is presented in table 4.3.

Table 4.3: Goodness of fit statistics for verifying model reliability

S/No	Goodness of Fit Statistics	Pb(II) ion Adsorption	Mn(II) ion Adsorption
1	R ²	0.9729	0.9287
2	Adj. R-Square	0.9459	0.8574
3	Pred. R-Square	0.8360	0.8122
4	Adeq. Precision	20.753	12.507
5	C.V %	2.90	3.66

It was observed from the result of table 4.3 that; there is a reasonable agreement between the predicted R² and the adjusted R² value. This reasonable agreement shows the adequacy of the second order polynomial equation.

Based on the goodness of fit statistics presented in table 4.3, a second order polynomial equation was generated as presented in equation 4.1 and 4.2 respectively

$$\begin{aligned}
 Y_{lead} = & 82.39333 - 0.32271X_1 + 2.71094X_2 - 2.00521X_3 + 0.055599X_4 - 0.017656X_1X_2 \\
 & + 0.44531X_1X_3 + 4.72656E - 003X_1X_4 + 0.97266X_2X_3 - 3.80859E - 003X_2X_4 \\
 & + 0.099284X_3X_4 - 0.032198X_1^2 - 0.19499X_2^2 - 15.12370X_3^2 - 5.78252E - 004X_4^2 \quad (4.1)
 \end{aligned}$$

where; X₁ = initial metal ion conc., X₂ = pH, X₃ = adsorbent dose, X₄ = contact time

$$\begin{aligned}
 Y_{manganese} = & 57.75667 + 0.45286X_1 - 1.65104X_2 + 2.8078X_3 + 0.086589X_4 + 0.15820X_1X_2 \\
 & - 0.056836X_1X_3 - 7.32422E - 004X_1X_4 - 0.48828X_2X_3 + 0.062826X_2X_4 + 2.92969E - 004X_3X_4 \\
 & - 0.018245X_1^2 + 0.12370X_2^2 - 0.13704X_3^2 + 7.36943E - 005X_4^2 \quad (4.2)
 \end{aligned}$$

where; X₁ = initial metal ion conc., X₂ = adsorbent dose, X₃ = pH, X₄ = contact time

To diagnose the statistical properties of the model, the normal probability plot of residual presented in Figures 4.9a-b were employed.

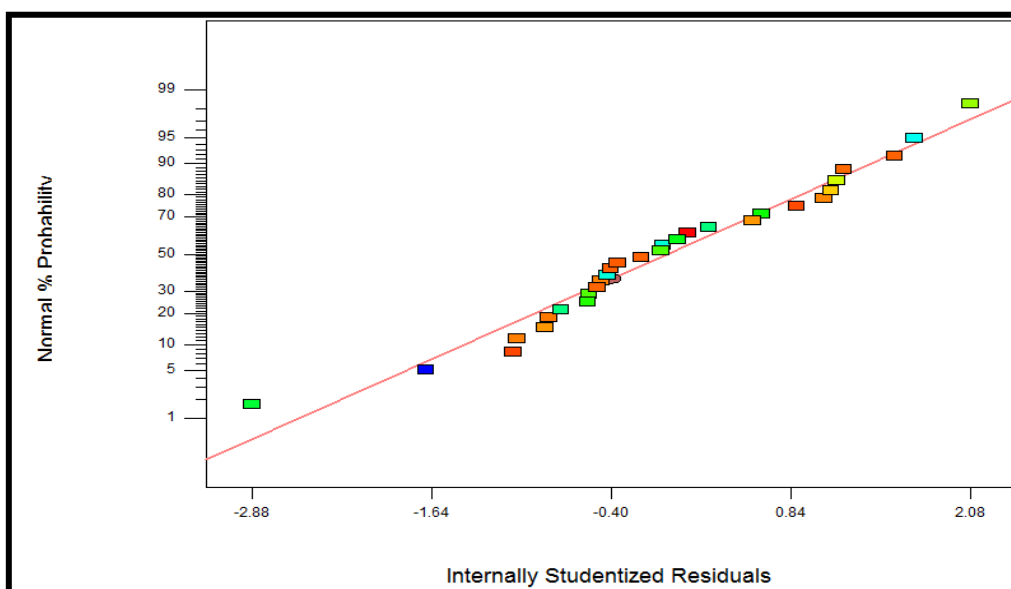


Figure 4.9a: Normal probability plot of studentized residuals for the adsorption of Pb(II) ion onto acid activated shale

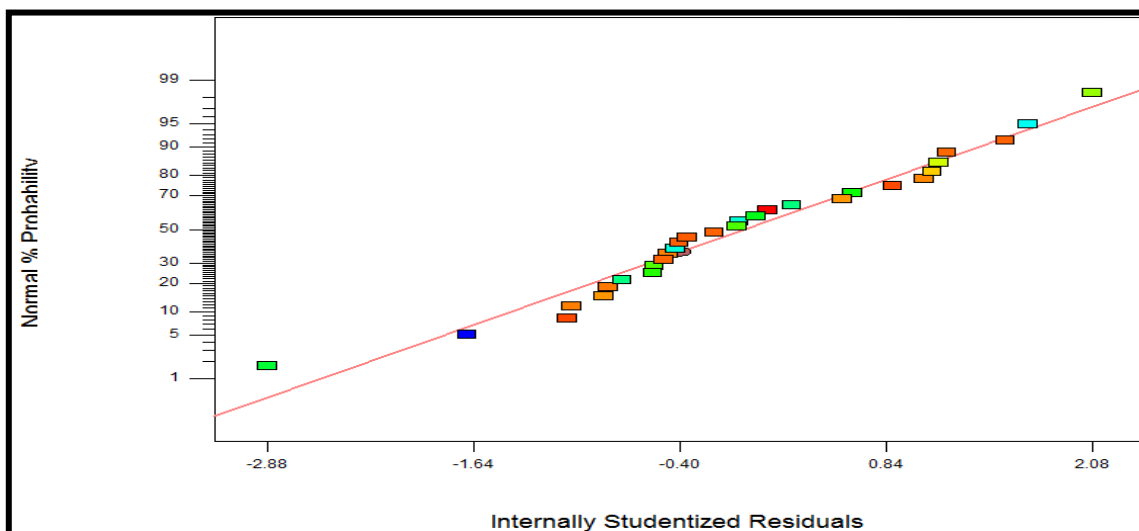


Figure 4.9b: Normal probability plot of studentized residuals for the adsorption of Mn(II) ion onto acid activated shale

The normal probability plot of studentized residuals was employed to assess the normality of the calculated residuals. The normal probability plot of residuals which is the number of standard deviation of actual values based on the predicted values was employed to ascertain if the residuals (observed – predicted) follows a normal distribution. It is the most significant assumption for checking the sufficiency of a

statistical model. Result of Figures 4.9a and 4.9b revealed that the computed residuals are approximately normally distributed an indication that the model developed is satisfactory. To study the effects of combine variables on the sorption efficiency of Pb(II) and Mn(II) onto acid activated shale, 3D surface plots presented as shown in Figure 4.10a-b were employed

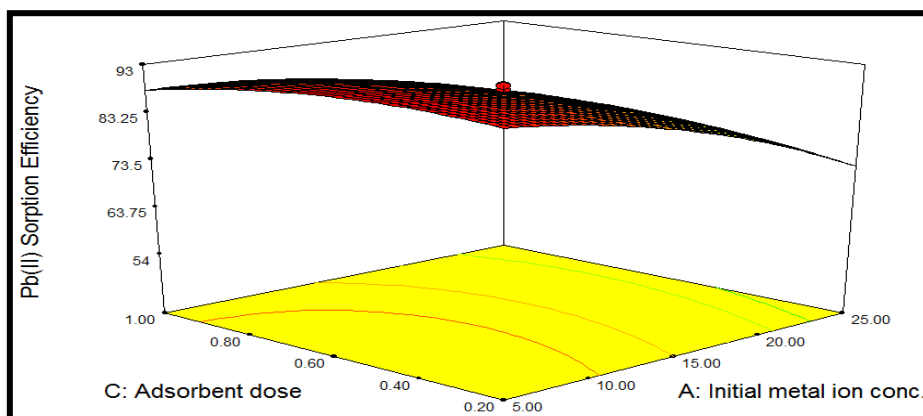


Figure 4.10a: Response surface plot showing the interaction between selected variables on Pb(II) ion adsorption onto acid activated shale

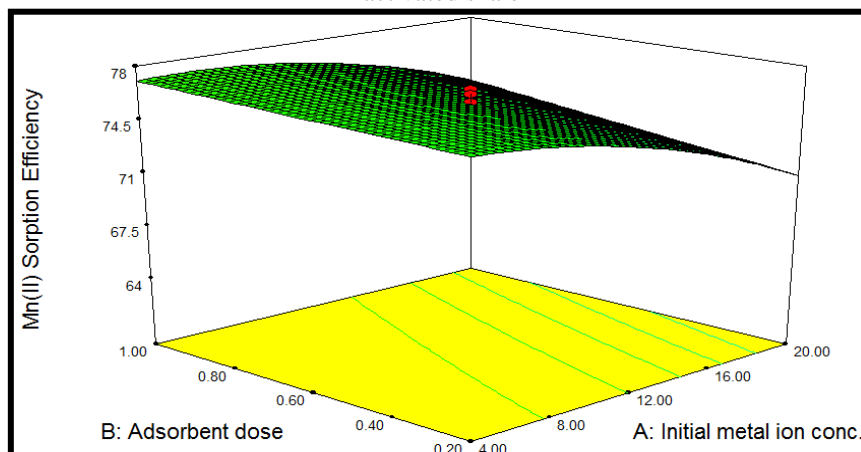


Figure 4.10b: Response surface plot showing the interaction between selected variables on Mn(II) ion adsorption onto acid activated shale

A closer look at Figure 4.10a-b shows the presence of a coloured hole at the middle of the upper surface. That was a clue that more points lightly shaded for easier identification fell below the surface. From the surface plots of Figures 4.10a and 4.10b, it was observed that the colour of the surface get darker towards initial metal ion concentration and indication that this variable strongly influenced the adsorption of Pb(II) and Mn(II) ions. The second order polynomial equations showing the relationship between the sorption efficiency (y) and the selected variables (x) as presented in equation 4.1 and 4.2 were thereafter solved to

$$Y_{lead} = 87.58 - 7.87A + 1.66B - 0.20C + 3.84D - 0.71AB + 1.78AC + 2.27AD + 1.56BC - 0.73BD + 1.91CD - 3.22AA - 3.12BB - 2.42CC - 1.33DD \tag{4.3}$$

$$Y_{manganese} = 75.64 - 2.27A + 0.80B + 0.84C + 6.14D + 0.51AB - 1.82AC - 0.28AD - 0.78BC + 1.21BD + 0.056CD - 1.17AA + 0.020BB - 2.19CC + 0.17DD \tag{4.4}$$

A (4 by 4) matrix from where the stationary point in terms of the selected input variables; initial metal ion concentration, pH, adsorbent dose, adsorption temperature and contact time

$$B_{lead} = \begin{bmatrix} -3.220 & -0.355 & 0.890 & 1.135 \\ -0.355 & -3.120 & 0.780 & -0.365 \\ 0.890 & 0.780 & -2.420 & 0.955 \\ 1.135 & -0.365 & 0.955 & -1.330 \end{bmatrix}$$

(Lead)

determine the optimum values of the process variables in enhancing the removal of Pb(II) and Mn(II) ions by acid activated shale. To solve the equation, two additional methods were employed to verify the numerical solution obtained from the experimental design software and they include; Genetic Algorithm (GA) and Inverse Matrix Method For the inverse matrix method, the second order polynomial equations were first written in terms of the coded value of the variables using the coefficient statistics of each metal ion studied as presented in equation 4.3 and 4.4 respectively.

were determined was then derived for each of the metal ion studied as presented below.

$$b_{manganese} = \begin{bmatrix} -7.870 & 0.255 & -0.910 & -0.140 \\ -1.170 & 0.020 & -0.390 & 0.605 \\ 1.660 & 0.200 & -0.390 & 0.605 \\ 0.200 & -0.910 & -2.190 & 0.028 \\ 3.840 & -0.140 & 0.605 & 0.028 & 0.170 \end{bmatrix}$$

(Manganese)

The product of the 4 by 4 matrix was solved using Microsoft Excel and the stationary point was determined as follows

$$\text{For Pb(II) ion; } -\frac{1}{2} B^{-1}b =$$

$$-\frac{1}{2} \begin{bmatrix} 3.801944 \\ -0.68686 \\ 2.058054 \\ 2.023574 \end{bmatrix} = \begin{bmatrix} -1.900972 \\ 0.34343 \\ -1.029027 \\ -1.011787 \end{bmatrix}$$

$$\text{For Mn(II) ion; } -\frac{1}{2} B^{-1}b =$$

$$-\frac{1}{2} \begin{bmatrix} -5.81719 \\ 3.49970 \\ -3.46849 \\ -3.48114 \end{bmatrix} = \begin{bmatrix} 2.90860 \\ -1.74985 \\ 1.73425 \\ 1.74057 \end{bmatrix}$$

The computed value of the stationary points (x_s) was substituted into equations 4.5, 4.6, 4.7, 4.8, 4.9 and 4.10 respectively to determine the optimum values of the selected variables while the efficiency of metal ion adsorbed expressed as percentage was calculated using equation 4.11

$$x_{conc} (Pb) = \frac{X_1 - 15}{5}, \tag{4.5}$$

$$x_{conc} (Mn) = \frac{X_1 - 12}{4} \tag{4.6}$$

$$x_{pH} = \frac{X_2 - 6}{2} \tag{4.7}$$

$$x_{temp} = \frac{X_3 - 298}{5} \tag{4.8}$$

$$x_{dose} = \frac{X_4 - 0.6}{0.2} \tag{4.9}$$

$$x_{time} = \frac{X_5 - 72}{24} \tag{4.10}$$

$$\hat{y} = \beta_0 + \frac{1}{2} x_s' b \tag{4.11}$$

To find the optimal solution using genetic algorithm, equation 4.3 and 4.4 were written in MATLAB codes using M-File and saved as (.m file) so as to generate the fitness function. Genetic algorithm tool box was then activated using 'gatool' command. Performance criteria selected for the algorithm include;

1. Double vector population type was selected since it works directly with the default creation mutation and crossover functions unlike custom population type that demands the writing of a new creation mutation and crossover functions.
2. The population size was set at 20 representing the number of individual in each generation. This size was chosen to allow the algorithm creates multiple subpopulation with each subpopulation working in synergy to obtain an optimum result
3. The creation function was set at uniform to allow the algorithm creates random initial population with a uniform distribution.
4. The initial population was left blank to allow the algorithm search and fix the best initial population
5. The initial scores were left blank to allow the algorithm use the fitness function to compute the most accurate initial population scores.
6. An initial range of [1 : 1.1] was set for the initial population
7. The default stochastic uniform selection function was used

8. Elite count of 2 and a crossover fraction of 0.8 was employed

Using the above performance criteria, the algorithm was lunched to perform the optimization in other to calculate the optimum values of the variables together with the graphical presentation of the current best individual among the variables and the average distance between individuals in each generation. The matrix form of GA solution is presented as follows

$$Pb(II) = \begin{bmatrix} 1.81800 \\ 0.36930 \\ 3.52581 \\ 0.21496 \end{bmatrix} \qquad Mn(II) = \begin{bmatrix} 0.24012 \\ 2.28037 \\ -1.8011 \\ 0.24938 \end{bmatrix}$$

The optimum value of the variables; initial metal ion concentration, pH, adsorbent dose, adsorption temperature and contact time were also computed using equations 4.5, 4.6, 4.7, 4.8, 4.9 and 4.10 respectively while the efficiency of metal ion adsorbed expressed as percentage was calculated using equation 4.11. The graphical presentation of the current best individual and the average distance between individuals per each generation are presented in Figures 4.11a-b

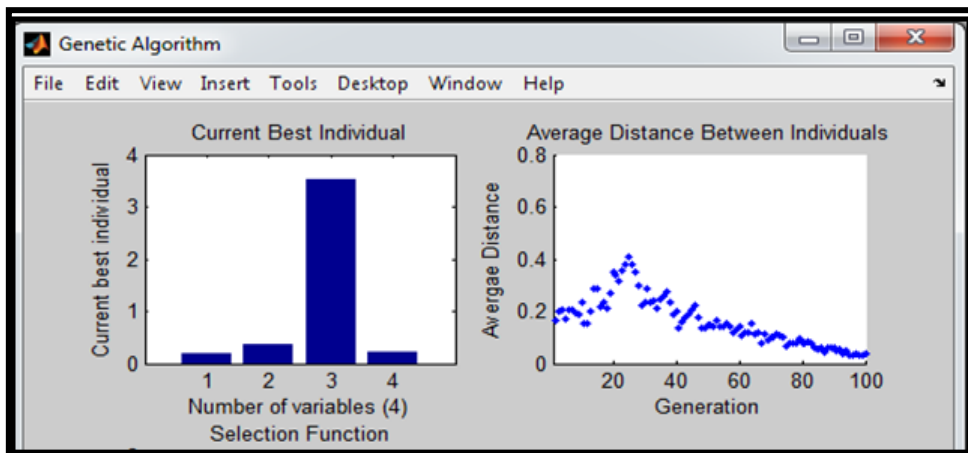


Figure 4.11a: Current best individual and the average distance for Pb(II) ion adsorption

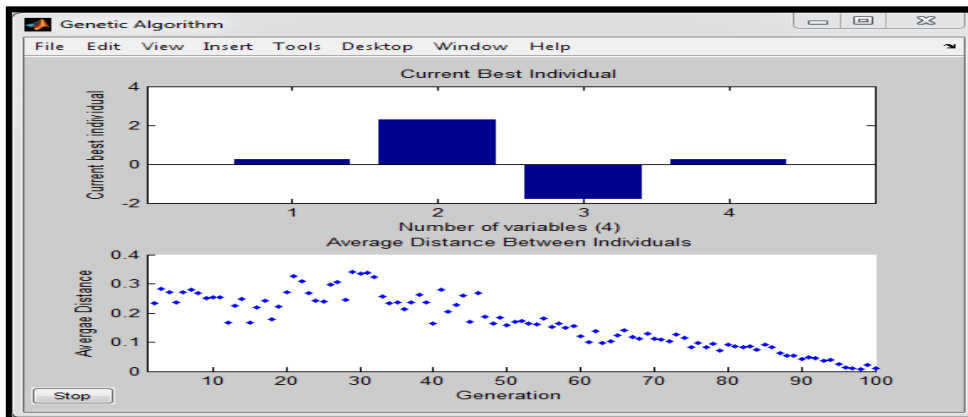


Figure 4.11b: Current best individual and the average distance for Mn(II) ion adsorption

Based on the results of Figures 4.11a and 4.11b, metal ion concentration was marked the best variable affecting the adsorption of Pb(II) and Mn(II) ions by acid activated shale. To validate the optimal solutions produced by the different

methods and select the optimum value of the variables, batch adsorption experiment was conducted based on the different solutions and the sorption efficiency of the metal ions were calculated and compared as shown in Table 4.4a.

Table 4.4a: Computed optimum values of adsorption variables based on different methods of optimization

Optimization Method	Variables	Optimum Values of Selected Variables		% Sorption Efficiency			
		Pb(II) ion Adsorption		Mn(II) ion Adsorption	Predicted	Experiment	Absolute Difference
Genetic Algorithm	Initial metal ion concentration (mg/l)	5.91		16.20	Pb(II) = 88.9	Pb(II) = 89.3	Pb(II) = 0.40
	pH	6.74		2.40	Cr(III) = 80.6	Cr(III) = 71.2	Cr(III) = 9.40
	Adsorbent dose (g)	1.03		1.06			
	Contact time (min)	77.16		77.99	Mn(II) = 76.6	Mn(II) = 46.7	Mn(II) = 29.9
	Adsorption temp. (K)	Nil		Nil			
Inverse Matrix Method	Initial metal ion concentration (mg/l)	5.50		23.63	Pb(II) = 84.0	Pb(II) = 83.8	Pb(II) = 0.20
	Adsorbent dose (g)	0.40		0.25	Cr(III) = 78.8	Cr(III) = 76.3	Cr(III) = 2.50
	Adsorption temp. (K)	Nil		Nil			
	Contact time (min)	48		114	Mn(II) = 80.3	Mn(II) = 74.3	Mn(II) = 6.00
	pH	6.69		9.47			
Numerical Optimization	Initial metal ion concentration (mg/l)	23.29		4.00	Pb(II) = 84.4	Pb(II) = 88.7	Pb(II) = 4.30
	Adsorbent dose (g)	0.89		1.00	Cr(III) = 78.8	Cr(III) = 77.4	Cr(III) = 1.40
	pH	6.97		7.74			
	Contact time (min)	120		120	Mn(II) = 85.3	Mn(II) = 88.7	Mn(II) = 3.40
	Adsorption temp. (K)	Nil		Nil			

From the results of Table 4.4, inverse matrix method had the least absolute difference between the predicted and experimental values and was therefore selected as the best solution to the optimal second order polynomial equation.

Based on the optimal solution generated by inverse matrix method of optimization, the calculated optimal values of adsorption variables for Pb(II) and Mn(II) ion adsorption onto acid activated shale is presented in Table 4.4b

Table 4.4b: Optimal values of adsorption variables

Optimization Method	Adsorption Variables	Calculated Optimal Values		
		Pb(II)		Mn(II)
Inverse Matrix Method	Initial metal ion concentration (mg/l)	5.50		23.63
	Adsorbent dose (g)	0.40		0.25
	Adsorption temp. (K)	Nil		Nil
	Contact time (min)	48		114
	pH	6.69		9.47

4.4 Modeling and prediction using modular neural network

data used for the neural network training is presented in Table 4.5

The descriptive statistics of the input and output

Table 4.5: Descriptive statistics of modular neural network variables

Variables	Data Statistics			
	Minimum	Maximum	Mean	Standard deviation
Input Layer				
Initial conc. of Pb(II) ion (mg/l)	4	35	14.21	8.029
pH	2	10	6.02	2.868
Adsorbent Dose (g)	0.2	1.0	0.593	0.3005
Contact Time (min)	24	120	70.93	35.050
Output Layer				
Pb(II) Sorption Efficiency (%)	54.6	92.3	77.074	9.453

To ascertain the most accurate training algorithm, different training algorithm were selected and tested to determine the best training algorithm that

will produce the most accurate network architecture. Table 4.6 shows the performance of the different algorithm tested.

Table 4.6: Selection of optimum training algorithm for modular neural network

S/No	Training Algorithm (Learning Rule)	Training MSE	Cross Validation MSE	R-Square
1	Gradient information (Step)	0.06578	0.04803	0.7495
2	Gradient and weight change (Momentum)	0.05895	0.04719	0.7726
3	Gradient and rate of change of gradient (Quick prop)	0.06234	0.04924	0.7483
4	Adaptive step sizes for gradient plus momentum (Delta Bar Delta)	0.02424	0.02692	0.8738
5	Second order method for gradient (Conjugate gradient)	0.02217	0.06828	0.7662
6	Improved second order method for gradient (Levenberg Marquardt)	0.00010*	0.00621*	0.988*

From the result of Table 4.6, it was observed that improved second order method for gradient also known as Levenberg Marquardt Back Propagation training algorithm was the best learning rule and was therefore adopted in designing the network architecture. To determine the exact number of hidden neuron, different numbers of hidden neurons were selected to train a network using the

Levenberg Marquardt Back Propagation training algorithm. The performance of the trained network was then assessed using mean square error (MSE) and coefficient of determination R^2 . The number of hidden neuron corresponding to the lowest MSE and the highest R^2 as presented in Table 4.7 was selected to design the network architecture

Table 4.7: Optimum number of hidden neurons for modular neural network

S/No	Number of Hidden Neurons	Training MSE	Cross Validation MSE	R-Square
1	2	0.000100*	0.006320*	0.988*
2	3	0.000105	0.011606	0.985
3	5	0.000100	0.063900	0.944
4	8	0.000105	0.107660	0.878
5	10	0.000104	0.221130	0.806

Based on the results of Table 4.6 and 4.7, Levenberg Marquardt Back Propagation training algorithm with 2 hidden neuron in the input and output layer with tangent sigmoid transfer function, having a target goal of 0.001 and epoch of 1000 was used to

train a network of 4 input processing elements (PEs), 1 output processing elements and 54 exemplars to produce an optimal neural network structure as presented in Figures 4.12a and 4.12b.

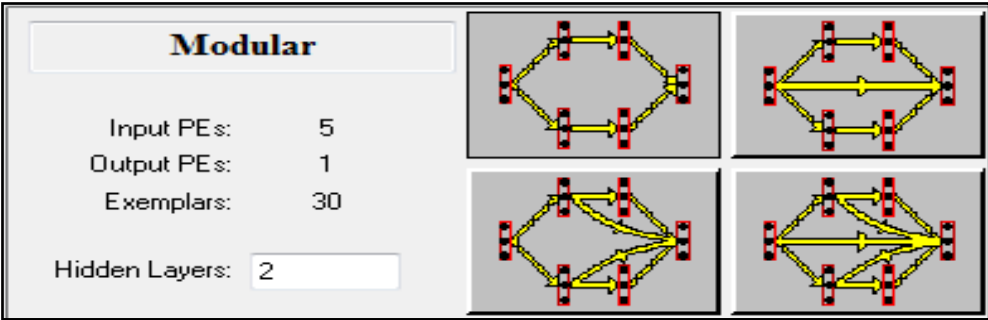


Figure 4.12a: Topology of MNN

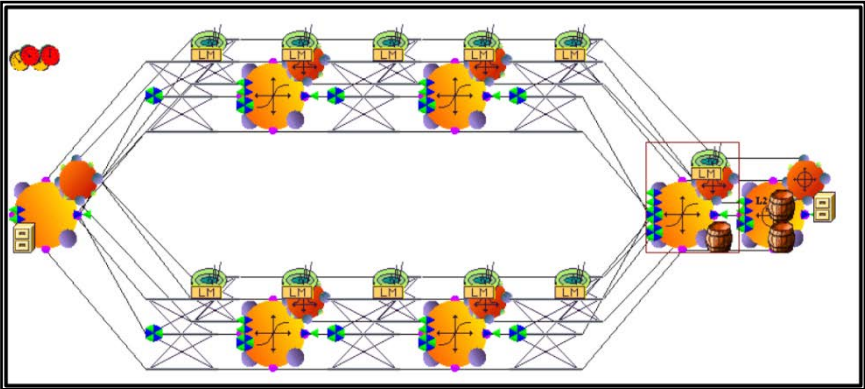


Figure 4.12b: Optimun network architecture

To assess the progress of the training, the mean square error (MSE) graph for training and cross validation presented in Figures 4.13a and 4.13b were obtained

The training and cross validation statistics which was employed to evaluate the effectiveness of the trained network is presented in figure 4.14

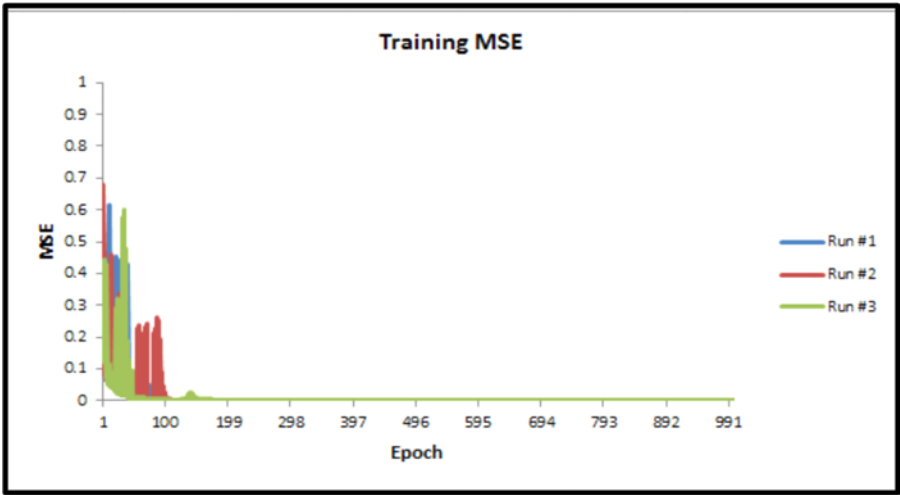


Figure 4.13a: Training progress of MNN

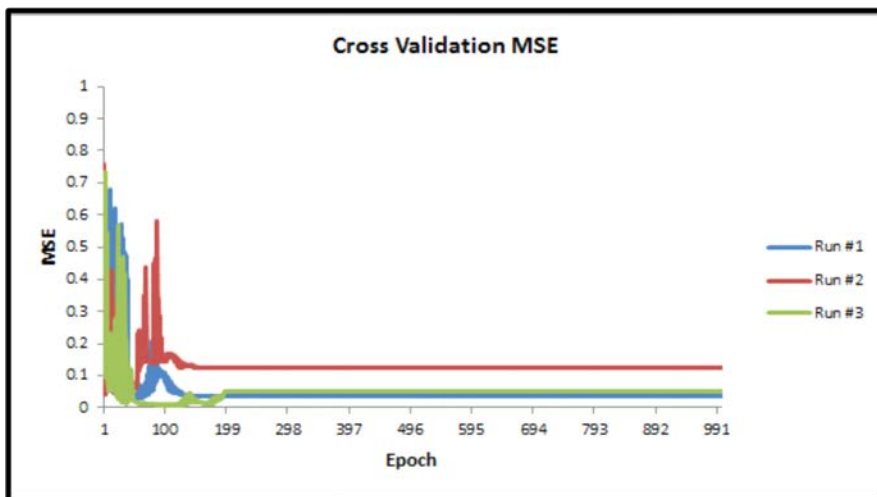


Figure 4.13b: Cross validation progress of MNN

<i>All Runs</i>	<i>Training Minimum</i>	<i>Training Standard Deviation</i>	<i>Cross Validation Minimum</i>	<i>Cross Validation Standard Deviation</i>
Average of Minimum MSEs	0.000104837	0	0.021899809	0.017056541
Average of Final MSEs	0.000104837	3.58365E-18	0.075534031	0.061351226

<i>Best Networks</i>	<i>Training</i>	<i>Cross Validation</i>
Run #	1	1
Epoch #	100	77
Minimum MSE	0.000104837	0.003058134
Final MSE	0.000104837	0.045040441

Figure 4.14: Evaluation statistics for MNN

To evaluate the performance of the trained network, comparison between the predicted sorption efficiency of Pb(II) ion onto acid activated shale using modular neural network (MNN) and the

experimental values of Pb(II) ion sorption efficiency by acid activated shale was obtained as presented in Figure 4.15

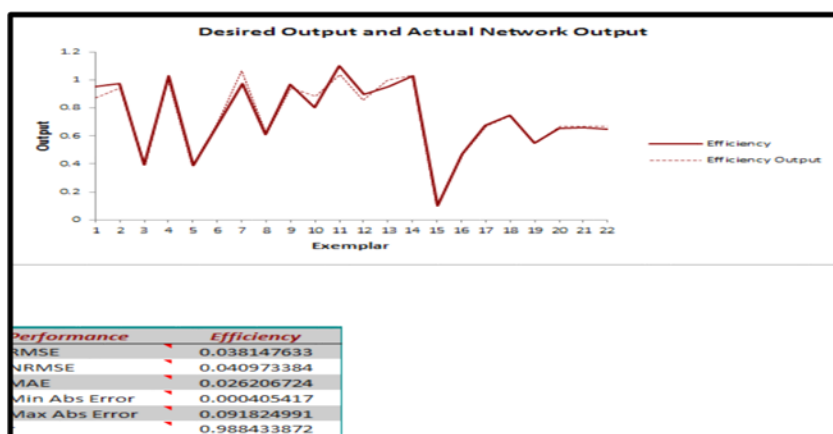


Figure 4.15: Comparison of predicted sorption efficiency of Pb(II) ion using MNN against the experimental values

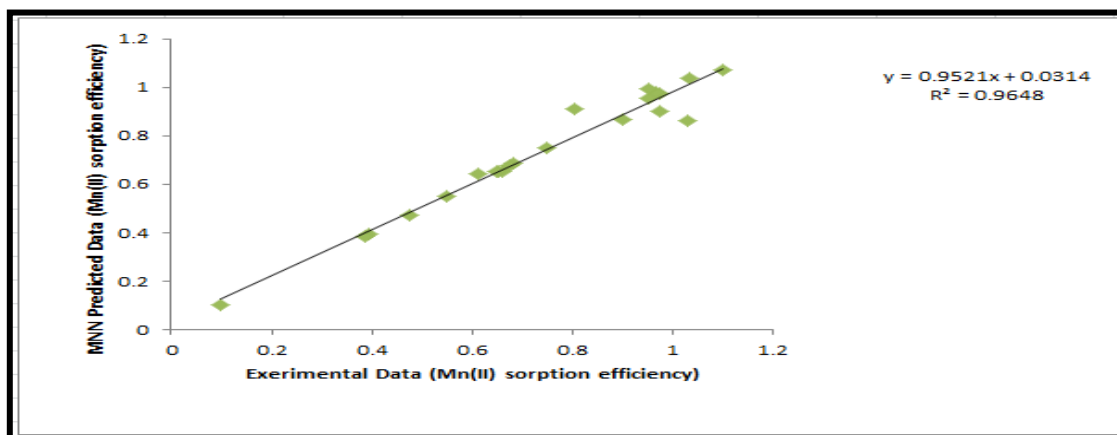


Figure 4.17: Performance of MNN on new input data

Result of figure 4.15 revealed a strong agreement between the experimental sorption efficiency data and modular neural network predicted data with a performance statistics of RMSE (0.03815), NRMSE (0.04097), Max.AE (0.02621), Min.AE (0.00041) and R^2 (0.988).

Sensitivity analysis was employed to give insights into the relative importance of individual input parameters in order to identify those parameters with the highest significant contributions towards the sorption of Pb(II) ion onto acid activated shale. Result of the sensitivity analysis is presented in Figure 4.16

Coefficient of determination of 0.9648 as observed in Figure 4.17 was good enough to justify the strength and accuracy of modular neural network as a tool for modeling and prediction of adsorption processes.

5. Conclusion

The study has successfully demonstrated the use of adaptive neuro-fuzzy inference system (Anfis) in ranking selected adsorption variables in terms of their significant contributions towards the effective removal of metal ions from aqueous solution. In addition, the performance of numerical optimization, inverse matrix method, and genetic algorithm in obtaining the optimal solution of the second order polynomial equation generated from statistical design of experiment has been successfully implemented. The approach will not only encourage the use of DOE in adsorption process, it will also expose researchers in the field of environmental systems optimization to new methods of optimal solution determination. More also, the suitability of modular neural network in modeling and prediction of metal ion adsorption onto porous solid adsorbent was investigated and found to be highly effective. Modular neural network gave a strong agreement between the experimental and predicted sorption efficiency of Pb(II) and Mn(II) ions with R^2 values of 0.977 and 0.9648 having performance statistics of RMSE (0.03815), NRMSE (0.04097), Max.AE (0.02621), Min.AE (0.00041) and R^2 (0.988).

References

- [1]. Lalvani, S.B.; Wiltowski, T., and Weston, A., (2010), Metal ions removal from wastewater by adsorption, Journal of Engineering Science, Vol. 2, pp 877-879
- [2]. Ong, S.; Seng, C., and Lim, P., (2007), Kinetics of adsorption of copper (II) and cadmium (II) from aqueous solution on rice husk and modified rice husk, Electronic Journal of Environmental Agriculture and food Chemistry, Vol. 6(2), pp 1764-1774.
- [3]. Kumar, N.K; Reddy, D.S.R and Venkateswarlu, P (2010), Application of response surface methodology for optimization of chromium biosorption from aqueous solution onto Syzigium Cumini (Java) seed powder, Microbial and Biochemical Technology, vol. 2(1), pp; 020-027
- [4]. Lima, E.C; Betina, R; Vagheti, J.C.P; Brasil, J.L; Nathalia, M.S; Dos-Santos Jr., A.A; Pavan, F.A; Silvio, L.P.D; Edilson, V.B and Da-Silva, E.A (2007), Adsorption of Cu(II) on Araucaria Augustifolia wastes; determination of the optimal conditions by statistical design of experiment, Journal of Hazardous Materials, vol. 140(1), pp; 211-220
- [5]. Lin, S. H., and Juang, R.S., (2002), Heavy metal removal from water by sorption using surfactant-modified montmorillonite, Journal of Hazardous Materials, vol. B92, pp 315 – 322
- [6]. Weng, C.H; Tsai, C.Z; Chu, S.H and Sharma, Y.C., (2007), Adsorption characteristics of copper (II) onto spent activated clay, Separation Purification Technology Journal, vol. 54, pp; 187-197
- [7]. Sinan, M.T; Beytullah, E and Asude, A (2011), Prediction of adsorption efficiency for the removal of Ni(II) ions by zeolite using artificial neural network (ANN) approach, Fresenius Environmental Bulletin, vol. 20(12), pp; 3158-3165
- [8]. Mohammed, Y; Farahnaz, E.B; Sepideh, K.B; Bahador, D.J; Soraya, H; Mohammad, R.M and Lugman, A.C (2013), Removal of Ni(II) from aqueous solution by an electric arc

furnace slag using artificial neural network (ANN) approach, *Advance in Environmental Biology*, vol. 7(9), pp; 2303-2310

[9]. Abdoliman, A; Ali, A.A and Fatemeh, A (2013), A study of cadmium removal from aqueous solution by sunflower powder and its modeling using artificial neural network (ANN), *Iranian Journal of Health Sciences*, vol. 1(3), pp; 28-34

[10]. Abhishek, K; Kumar, R.R; Jyoti, K.A and Shalini, S (2011), ANN modeling on prediction of biosorption efficiency of Zea Maize for the removal of Cr(III) and Cr(VI) from wastewater, *International Journal of Mathematics Trends and Technology*, July/August Issue, pp; 23-29

[11]. Cerino-Cordova, F.J; Garcia-Leon, A.M; Garcia-Reyes, R.B; Garza-Gonzalez, M.T; Soto-Regalado, E; Sanchez-Gonzalez, M.N and Quezada-Lopez, I (2011), Response surface methodology for lead biosorption on *Aspergillus Teseus*, *International Journal of Environmental Science and Technology*, vol. 8(4), pp; 695-704

[12]. Animesh, D. (2013), Modular approach to big data using neural network, unpublished M.Sc. dissertation submitted to the department of computer science, San Jose State University, pp 23.56.

[13]. Mariadas, K.; Kalyani, G.; Joga, H.R.; Kumar, P. Y and King, P., (2012), The removal and equilibrium studies of cadmium by natural clay as adsorbent, *International Journal of Scientific Engineering Research*, Vol. 3(8), pp 1-6

[14]. Krishna, G.B and Susmita, S.G (2006), Adsorption of chromium (VI) from water by clays, *Industrial Engineering and Chemical Resource Journal*, vol. 45, pp; 7232-7240

[15]. Hao, C and Wang, A., (2007), Kinetic and isothermal studies of lead ion adsorption onto polygorskite clay, *Journal of Colloid and Interface Science*, vol. 307, pp 309 – 316

[16]. Badmus, M.A.O.; Audu T.O.K and Anyata, B.U, (2007), Removal of lead ion from industrial wastewaters by activated carbon prepared from periwinkle shells, *Turkish Journal of Engineering and Environmental Science*, pp; 251 – 263

[17]. Gimbert, F.; Morin-Crini, N.; Renault, F.; Badof, P.M and Crini, G., (2008), Adsorption isotherm models for dye removal by cationized starch-based materials in a single component system; Error analysis, *Journal of Hazardous Materials*, Vol. 157, pp 34-46

[18]. Gunay, A.; Arslankaya, E and Tosun, I., (2007), Lead removal from aqueous solution by natural and pretreated clinoptilolite; adsorption equilibrium and kinetics, *Journal of Hazardous Materials*, Vol. 146, pp 362-371

[19]. Hong, Z.; Donghong, L.; Yan, Z.; Shuping, L., and Zhe, L., (2009), Sorption isotherm and kinetic modeling of aniline on Cr-bentonite, *Journal of Hazardous Materials*, vol. 167, pp 141 – 147

[20]. I.R. Ilaboya; E.O. Oti; G.O. Ekoh and L.O. Umukoro (2013); Performance of activated carbon from cassava peels for the treatment of effluent wastewater, *Iranica Journal of Energy & Environment (IJEE)*, an Official Peer Reviewed Journal of Babol Noshirvani University of Technology, vol. 4 (4), pp: 361-375

[21]. Abdullah, A.H; Anuark, P; Zulkarnain, Z; Mohd, Z.H; Dzulkefly, K; Faujan, A and Ong, S.W (2001), Preparation and characterization of activated carbon from gelam wood bark (*Melaleuca Cajuputi*), *Malaysian Journal of Analytical Science*, vol. 7(1), pp; 65-68

[22]. Arenas, L.T; Vagheti, J.C.P; Moro, C.C; Lima, E.C; Benvenuti, E.V and Costa, T.M.H (2004), Dabco/silica sol-gel hybrid material; the influence of the morphology on the CdCl₂ adsorption capacity, *Materials Letters*, vol. 58 pp; 895-898